The friction of wrinkles

Hamid Mohammadi[1] and Martin H. Müser[2]

[1]*Dept. of Applied Mathematics, University of Western Ontario, London, Ontario, Canada N6A 5B6*
[2]*FBR Materialwissenschaften, Universität des Saarlandes, 66123 Saarbrücken, Germany*

Sufficiently thin elastic sheets wrinkle when they are in contact with a small adhesive counterbody. Despite significant progress on the dynamics of wrinkle formation and morphology, little is known about how wrinkles impede the relative sliding motion of the counterbody. Using molecular dynamics we demonstrate that instabilities are likely to occur during sliding when the wrinkle pattern has asymmetries not present in the counterbody. The instabilities then cause Coulomb's friction law. The behavior can be rationalized in terms of simple models for multistable elastic manifolds.

Thin elastic sheets wrinkle, similar to the way rods buckle, whenever a compressive stress acting on them exceeds a critical value.[1–4] Wrinkles occur in sheets whose thickness is much smaller than their in-plane dimensions, be it in a system as large as a tectonic plate or in a few nanometer thick, crosslinked elastomer resting on a soft foundation. The origin of the wrinkle inducing stress does not necessarily have to be mechanical (pinched skin) but can also be chemical in nature (aging skin). Wrinkling plays an increasingly important role in a variety of technologies, for instance, in the search for new ways to pattern surfaces for optical[5] and electronic applications[4,6] as well as for material characterization.[3,4] Recent work was particularly focused on the dynamics of wrinkle formation[7–9] and the control of wrinkle patterns.[10–12] Nevertheless, little is known about the dynamic response of wrinkles to time-dependent stresses.

In their classical paper on the origin of wrinkles in biological systems, Harris *et al.*[13] argued that traction forces between tissue cells and thin sheets of chemically inert silicone rubber cause wrinkles in the rubber and not the other way around. Their experiments dismissed the previously-held believe that the formation of wrinkles require protein networks to be become dehydrated. Today, it is well established that neither dehydration nor strong local adhesions are needed for wrinkles to occur in thin elastic sheets, as evidenced most clearly by wrinkle that water drops induce in thin, freely floating elastomeric films.[14] Likewise, the presence of friction - as observed for the much investigated keratocytes on silicon rubber[15] - may not require local adhesions either.

Wrinkle-related friction studies avoiding local adhesions have so far been performed on soft elastomers, which had been molded such that their shapes resembled those of originally flat, unmolded elastomers wrinkling in response to a static compression.[16] These experiments produced the insight that the structured surfaces had lower friction than unstructured ones. Yet, they do not answer the question if externally-driven wrinkles will result in hysteretic wrinkle dynamics, when wrinkles are not frozen in. Hysteresis, however, entails the loss of energy - or friction, Depending on the nature of the instabilities creating the hysteresis, a different rate or velocity dependence of friction can be found.[17] Any quasi-discontinuous dynamics should induce Coulomb's law of friction, i.e., a weak velocity dependence.

In this Letter, we will mainly be concerned with the question if the velocity dependence of friction changes qualitatively at the point where the thickness of the manifold becomes sufficiently small so that the adhesive counter body induces wrinkles. For this purpose, we will use molecular dynamics, which has been established to reproduce both experiments and scaling hypotheses on the buckling and crumpling of membranes.[18]

Our model consists of a particle adsorbed on a square, elastic manifold, which is is composed of discrete grid points ("atoms") that are connected with elastic springs. The adsorbed particle has the quasi-spherical topology of a C_{60} molecule, unless mentioned otherwise. All units in this paper are expressed in terms of the mass of a manifold atom, the stiffness of springs connecting two in-plane adjacent manifold atoms, and the equilibrium spacing between them. The effective thickness t of the membrane is controlled by multiplying the stiffness of springs that do not lie completely within the xy-plane with a scaling factor t. Simulations are conducted with a self-written molecular dynamics code. More details can be found in the auxiliary material.

We would first like to demonstrate that our model produces the proper response of the manifold to an adhesive counter body as a function of its thickness, see Fig. 1. At large thickness, grooves occur. They are elastic deformations in response to the periodic boundary conditions and thus exhibit the four-fold symmetry of a square. As these grooves can be interpreted as simple field lines connecting adjacent adsorbed particles, we classify this regime as unwrinkled. Around $t = 1$ "real" wrinkles start occurring, i.e., patterns that deviate from trivial symmetry. When the manifold becomes thinner, the number of wrinkles increases and their depth decreases, conforming to the known properties of wrinkles[4]. In addition, wrinkles are starting to be no longer symmetrically equivalent for thicknesses well below unity, e.g. Fig. 1(c). The movie wrinkling3.mpg presented in the auxiliary electronic material shows the deposition of a particle onto the substrate and the subsequent wrinkle formation dynamics.

Configurations obtained during sliding differ from those where no external forces act on the adsorbed particle. This claim is substantiated in Fig. 1(d) depicting the system in which an adsorbed particle had been slid

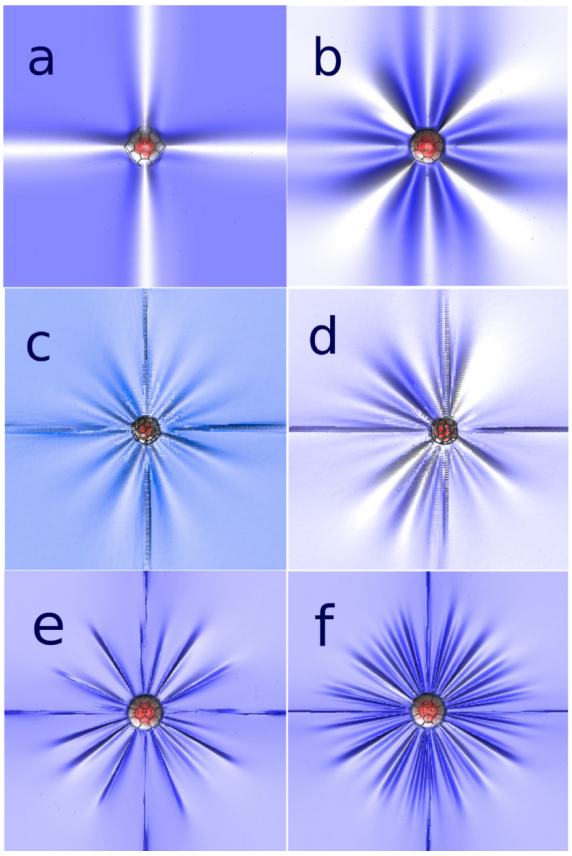

FIG. 1: (Color online.) Top view on the elastic manifold for various thicknesses t: (a) 100, (b) 1, (c) 0.1 (d) and (e) 0.01, and (f) 10^{-3}. In all graphs, patterns are shown after the particle is deposited, except in figure (d), where the adsorbed particle has been slid by a few lattice constants to the right with a velocity of 0.256×10^{-3} in reduced units.

by a few lattice constants. This configuration lacks the inversion symmetry about the plane normal to the sliding direction. Non-sliding systems always assume inversion symmetry after thermal averaging. The way in which symmetry is broken in Fig. 1d resembles that of keratocytes moving on highly compliant silicon rubber, see for example Fig. 6a in Ref. [15]. Specifically, more wrinkles are found behind the moving particle than in front of it.

As is the case for any finite adsorbed (stable) particle, there exists a well-defined linear response of the drag velocity v to an external driving force F in the limit of small F, i.e., $v = F/(m\gamma)$, where m is the mass of the adsorbed particle and γ is the drag coefficient or the inverse slip time.[19] A question that we are interested in is whether there is a change in γ as wrinkles start to form. As discussed in more detailed in the auxiliary material, drag coefficients can be determined in thermal equilibrium either through measurements of the particle's thermal diffusion constant, or alternatively, by acquiring and integrating over the time autocorrelation function of the force (FACF), $\langle F_x(\tau)F_x(0)\rangle$, where $F_x(\tau)$ is the force at time τ acting between manifold and particle. In Fig. 2 we report our results for the drag coefficient.

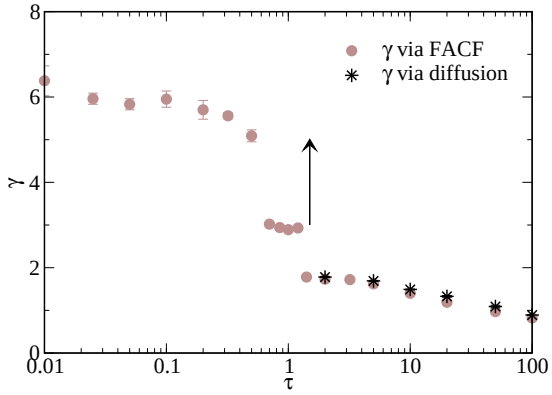

FIG. 2: Drag coefficient γ of the adsorbed particle as determined by (a) integration of the force autocorrelation function (circles) and (b) measurement of the diffusion constant (stars). For $t < 2$ only upper bounds in the diffusion constants and thus lower bounds for γ could be determined. The latter lie outside of the shown domain, as indicated by the arrow.

In the unwrinkled regime, the FACF and diffusion constant based methods both produce similar estimates for γ. This no longer holds for thicknesses $t < 1$, where wrinkles occur in addition to those connecting an adsorbed particle with its closest images. There the employed 10^7 time steps no longer suffice to measure meaningful diffusion constants. The reason is that the adsorbed particle, which is kept at a thermal energy of $T = 10^{-4}$, is pinned - or at best sub-diffusive - within the given time window. From such simulations, only upper bounds for the diffusion constant can be obtained. The resulting lower bounds for γ still exceed the domain chosen for Fig. 2. Since the particles appear pinned at $t < 1$, the values of γ as obtained by the FACF can be interpreted as an (instantaneous) damping that the adsorbed particle experiences while the system is arrested in one basin of the potential energy surface. This instantaneous damping shows a second quasi-continuous change near a critical value of $t \approx 0.4$ and keeps increasing as the thickness decreases. This second transition coincides with another qualitative morphological change during which wrinkles become symmetrically distinct, i.e., their widths and lengths no longer take essentially unique values for a given system.

The observed pinning of an adsorbed particle at small thicknesses may appear counterintuitive if one considers the elastic manifold to be continuous. However, the discreteness of the manifold breaks its perfect translational invariance, thereby allowing (quasi-static) shear forces to be exerted. A similar phenomenon is known from the spreading of liquid droplets on surfaces, where heterogeneities can pin contact lines and induce contact angle hysteresis. This is why rain drops do not necessarily run down a seemingly flat, inclined glass surface.[20]

Pinning implies static friction and in most cases also Coulomb friction once sliding has been initiated. In our analysis, we focused on kinetic friction, because static friction (that is the first stiction peak) turned out to be undesirably sensitive to the initial conditions. Conversely, kinetic friction had substantially less history dependence once the particles had been slid a few lattice constants. We calculated kinetic friction as a function of sliding velocity for two thicknesses ($t = 10^{-3}$ and $t = 10$), see inset of Fig. 3, and as a function of thickness for a fixed relative center of mass velocity of $v = 0.256 \cdot 10^{-3}$, see main part of Fig. 3. In all these simulations, we reduced the temperature by a factor of ten as compared to the simulations in thermal equilibrium, so that even those instabilities could be captured that only involved small energies.

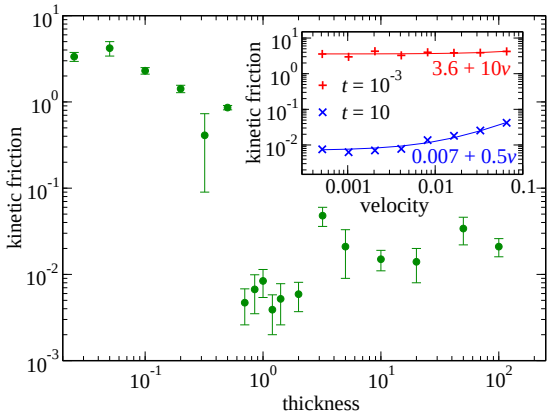

FIG. 3: (Color online.) Main figure: Kinetic friction obtained at $T = 10^{-5}$ for different thicknesses. Inset: Kinetic friction as a function of the sliding velocity v for two different thicknesses: $t = 10^{-3}$ (wrinkled regime) and $t = 10$ (unwrinkled). Lines are linear fits to the data.

The extremely weak velocity dependence of kinetic friction for the thin substrate is indicative of Coulomb friction and thus consistent with the observation that an undriven particle was pinned. The large difference in kinetic friction, almost three orders of magnitude, between the $t = 10^{-3}$ and the $t = 10$ thick elastic manifolds implies that the kinetic friction with the thinner manifold cannot simply be related to local adhesions. The small but seemingly finite friction in the limit of small velocities for the thick sheet is due to local instabilities that do not significantly affect the wrinkle morphology. The linear response regime could not be reached in the calculations shown in Fig. 3, because very small temperatures had been chosen in these runs.

The non-equilibrium simulations also show three thickness regimes that roughly coincide with those obtained in the thermal-noise calculations. Dissipation is again largest for the thinnest manifolds, this time by orders of magnitude. However, the intermediate regime shows less kinetic friction than the large thickness regime, which differs from the trends in the calculations without external driving. The reason for the different behaviors lies in the different morphologies that the adsorbed C_{60} shaped particle can induce in the substrate. Specifically, the wrinkles in the large t regime had always four-fold symmetry, while for intermediate values of t, the symmetry was eight-fold in the thermal-noise simulation, which quickly converted to three-fold symmetry once sliding had begun. Preliminary runs of particles with different shapes, i.e., one monomer with large Lennard Jones radius, and one flat heptagon, have not shown any sign of an intermediate regimes.

The arguably most interesting effect in Fig. 3 is the increase in the friction force by a factor of more than 100 as the thickness is decreased from $t = 0.7$ to $t = 0.5$. To elucidate the origin of this behavior, lateral forces are shown as a function of slid distance Δx in Fig. 4(a). The lateral force of the thicker substrate has various instances in time, for example at a slid distance of $\Delta x \approx 5.75$, where it changes rather quickly with Δx. Yet, once steady state has been reached (after going through one single "stiction peak" at the early stages of sliding after deposition - not shown here) the lateral force apparently evolves rather smoothly in time for $t = 0.7$. This is why dissipation is small. Conversely, the slightly thinner sheet produces a distinct saw-tooth time dependence, which is indicative of instabilities or stick-slip type motion within the system leading to large dissipation. For even thinner substrates, this stick slip motion becomes erratic and is no longer periodic with the manifold lattice (see also the movie sliding.mpg on stick slip motion in the auxiliary electronic material).

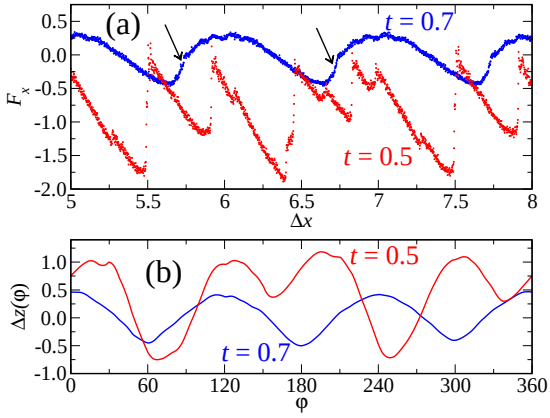

FIG. 4: (Color online.) (a) Instantaneous force F_x as a function of the slid distance Δx for two different thicknesses. Arrows mark points where the thicker substrate is close to showing slips. (b) Height of the manifold at a distance twice the diameter of the adsorbed particle for the same thicknesses.

The discontinuous increase in friction when the manifold thickness decreases from $t = 0.7$ to $t = 0.5$ coincides with a morphological change of the manifold. The $t = 0.7$ has three highly symmetric wrinkles, shown in Fig. 4(b), while the slightly thinner sheet has one more wrinkle and

probably more important, wrinkles now are inequivalent. This asymmetry of the pattern is not an immediate consequence of the shape of the adsorbed body. We made the same observations in the two sets of test runs in which either a large Lennard Jones monomer or a flat heptagon had been used as adsorbed particles. The asymmetry of the wrinkle pattern is significant because it implies that there are several mechanically (meta)stable configurations that cannot be reached from one another without changing the energy of the system. For example, making the $t = 0.5$ wrinkles at $\varphi \approx 160^\circ$ and 340° as deep as those at $\varphi \approx 70^\circ$ and 250° and vice versa will require the system to pass over an energy barrier.

The multistability of discrete, elastic systems has long been recognized as a possible origin of energy-dissipating instabilities leading to Coulomb's friction law:[21,22] Once a configuration becomes unstable, the degrees of freedom quickly advance to the vicinity of another energy minimum. Multistability however do not arise automatically in discrete elastic systems. Whether instabilities occur can depend on details such as the ratio of atomic spacings in adsorbed layer and substrate as well as on other details of the interaction. These and related insights have been best formalized in the context of the Frenkel Kontorova model.[23]

It is certainly not surprising that thinner sheets exhibit a higher propensity for instabilities to occur than thick sheets due to their higher compliance. Other studies show the same trends, be it layers of graphite lubricating nano-scale objects[24], the buckling hysteresis in multiwalled carbon nanotubes under cyclic compression[25], the snap transitions in adhesion between a shell and a substrate (which do not require asymmetry in the wrinkle pattern!),[26] or scaling theories of friction of elastic manifolds as a function of their physical dimension.[27] In this sense there is no new wrinkle in the theory of friction on a fundamental level but a matured understanding of the mechanisms that can lead to it.

MHM gratefully acknowledges financial support from NSERC. Simulations were run on Sharcnet.

[1] M. A. Biot, Proc. R. Soc. London, Ser. A **242**, 444 (1957).
[2] L. D. Landau and E. M. Lifshitz, *Elasticity Theory* (Nauka, Moscow, 1965).
[3] E. Cerda and L. Mahadevan, Phys. Rev. Lett. **90**, 074302 (2003).
[4] J. Genzer and J. Groenewold, Soft Matter **2**, 310 (2006).
[5] C. Harrison, C. M. Stafford, W. Zhang, and A. Karim, Appl. Phys. Lett. **85**, 4016 (2004).
[6] D. H. Kim, J. H. Ahn, W. M. Choi, H. S. Kim, T. H. Kim, J. Song, Y. Y. Huang, Z. Liu, C. Lu, and J. A. Rogers, Science **320**, 507 (2008).
[7] N. Sridhar, D. J. Srolovitz, and Z. Suo, Appl. Phys. Lett. **78**, 2482 (2001).
[8] R. Huang and S. H. Im, Phys. Rev. E **74**, 026214 (2006).
[9] S. H. Im and R. Huang, J. Mech. Phys. Solids **56**, 3315 (2008).
[10] X. Chen and J. W. Hutchinson, ASME J. Appl. Mech. **71**, 597 (2004).
[11] Z. Huang, W. Hong, and Z. Suo, J. Mech. Phys. Solids **53**, 2101 (2005).
[12] H. T. Evensen, H. Jiang, K. W. Gotrik, F. Denes, and R. W. Carpick, Nano Lett. **9**, 2884 (2009).
[13] A. K. Harris, P. Wild, and D. Stopak, Science **208**, 177 (1980).
[14] J. Huang, M. Juszkiewicz, W. H. de Jeu, E. Cerda, T. Emrick, N. Menon, and T. P. Russell, Science **317**, 650 (2007).
[15] K. Burton, J. H. Park, and D. L. Taylor, Mol. Biol. Cell **10**, 3745 (1999).
[16] C. J. Rand and A. J. Crosby, J. Appl. Phys. **106**, 064913 (2009).
[17] M. H. Müser, Phys. Rev. Lett. **89**, 224301 (2002).
[18] J. A. Åström, J. Timonen, and M. Karttunen, Phys. Rev. Lett. **93**, 244301 (2004).
[19] H. Risken, *The Fokker Planck equation* (Springer, Heidelberg, 1984).
[20] L. Leger and J. F. Joanny, Rep. Prog. Phys. **55**, 431 (1992).
[21] L. Prandtl, Z. Angew. Math. Mech. **8**, 85 (1928).
[22] M. H. Müser, M. Urbakh, and M. O. Robbins, Adv. Chem. Phys. **126**, 187 (2003).
[23] O. M. Braun and Y. S. Kivshar, Phys. Rep. **306**, 2 (1998).
[24] C. Lee, Q. Y. Li, W. K. abd X. Z. Liu, H. Berger, R. W. Carpick, and J. Hone, Science **328**, 76 (2010).
[25] H. W. Yap, R. S. Lakes, and R. W. Carpick, Nano Lett. **7**, 1149 (2007).
[26] R. M. Springman and J. L. Bassani, J. Mech. Phys. Solids **56**, 2358 (2008).
[27] M. H. Müser, Europhys. Lett. **66**, 97 (2004).